Design and Implementation of Model Predictive Control for Parallel Distributed Energy Resource in Islanded AC Microgrids

Design and Implementation of Model Predictive Control for Parallel Distributed Energy Resource in Islanded AC Microgrids.

Hussain Sarwar Khan
School of Technology and Innovations
University of Vaasa
Vaasa, Finland
Hussain.khan@uwasa.fi

Jagdesh Kumar
School of Technology and Innovations
University of Vaasa
Vaasa, Finland
jagdesh.kumar@uwasa.fi

Kimmo Kauhaniemi
School of Technology and Innovations
University of Vaasa
Vaasa, Finland
kimmo.kauhaniemi @uwasa.fi

***Abstract*— This study proposes the voltage control strategy for distributed energy resource (DER) in islanded AC microgrids (MG). Typically, AC MG can maintain a constant voltage at the point of common coupling (PCC) as well as perform power-sharing among the DERs. However, linear controllers have several restrictions such as slow transient response, poor disturbance rejection capability etc. Therefore, this study presents an FCS-MPC for a DER with effective voltage regulation capability. The investigated work demonstrates excellent steady-state performance, a low computational burden, better response under transients and have low switching frequency as compared to linear control. First, the benefits of FCS-MPVC for single DER has been studied, then the same topology along with droop control is employed for multiple DERs in AC MG to serve the load. Droop control shows improved power-sharing among the DERs. The performance of the proposed control technique is demonstrated through MATLAB/Simulink simulations for single DG and AC MG under linear, non-linear loading conditions.**

Keywords*— Distributed Energy Resource (DER) Model Predictive Control (MPC); Primary Control of MG.

I. INTRODUCTION

Microgrids (MG) is one of the fundamental technologies which make the electrical grids more intelligent, flexible, and distributed and the incursion of distributed energy resources (DERs) is possible in electrical grids. MG is a localized cluster of adaptive loads, distributed energy storage, and distributed generation (DG) and has effective control. MG with installed DGs able to work in islanded and grid-connected (GC) mode or both. In GC mode, MG can be utilized to provide auxiliary services to power systems such as voltage support, peak load shaving, and load shifting [1, 2]. In the case of a power outage from the utility grid or low power quality, MG can seamlessly disconnect from the utility grid and pursue to provide high-quality power to load in standalone mode. The standalone mode can be further classified into two categories in the context of time. Temporary standalone mode occurs due to preplanned maintenance or due to spontaneous failure in transmission lines between MG and utility grid.

The permanent islanded mode is capable to supply power to remote communities, where energy from the electrical grid is not favourable [3]. In this study, permanent islanded MG is considered. Direct current (DC) MG has a more appealing feature in terms of efficiency, control, and simplicity than AC MG, but the wide majority of load requires ac supply [4]. Consequently, it is mandatory to establish ac MG architecture. AC and DC parts of MG is interfaced through voltage source converters (VSC) [5]. For critical load applications, paralleled connected VSCs operation present redundancy, high reliability, and flexibility. In many cases, it is effectively viable to distribute a high power load between several VSC despite using power devices with a high rating. Commonly, VSCs are connected parallelly to form AC MG.

For the parallel operation of multiple DGs in islanded mode, it is highly expedient to design a decentralized controller, i.e., no external communication network between VSC based DGs. Therefore, a droop control approach is commonly employed and serves as an outer loop. It produces a voltage reference that is delivered to the corresponding VSCs inner loop. The inner loop consists of a voltage compensation loop. The purpose of the voltage regulation loop is to compensate for the output voltage of VSC according to reference. For the voltage control loop of VSC in MG, a linear control along with pulse with modulation (PWM) is widely found in literature and vastly used by the power electronics industry. However, these control techniques have many practical restrictions, and they are incapable of reducing the steady-state error to zero and also had not the capacity to overcome the nonlinearity of the system [6]. Hysteresis control is a type of non-linear controller, it takes the error to zero within a few-cycle and has variable switching frequency, which produces severe stress on VSI switches. This stress decreases the life of the inverter [7, 8].

Finite control Set Model predictive control (FCS-MPC) is a digital control method, and its basic principle is different from linear control. It uses the discrete model of VSC along with its filter to determine the future behavior for all possible input combinations. One of the inputs, which have the least value of predefined cost function (CF) is selected to be applied for the next sampling instant instead of drafting a separate loop for each controlled variable and cascading them together as in linear control system. CF is a square of the Euclidean distance between controlled and reference signals. MPC with load current observer is presented in [9]. The control technique proposed in [9] is quite simple, but the total harmonic distortion (THD) of the output voltage is high. In [10], predictive control is presented, and the author has not investigated the performance

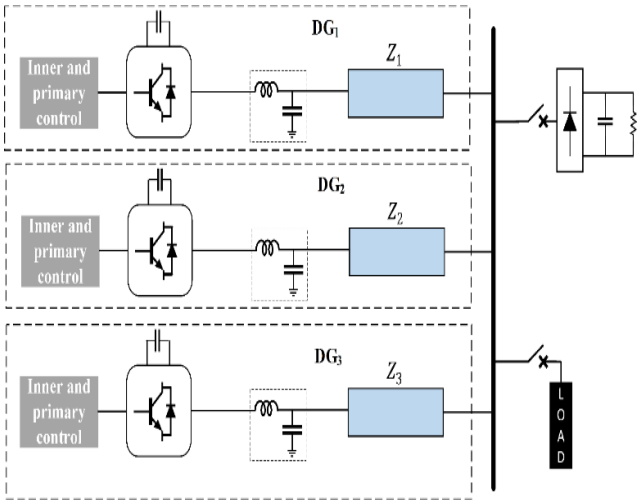

Figure 1. Islanded MG contains Three DG's with VSI and different type of loads.

of the control technique for the non-linear load. The robustness, exemplary transient behavior and easy inclusion of non-linearities make the FCS-MPC the best alternative for the control of power converters [11].

This paper presents a robust voltage control approach for VSC to control the output voltage of single and also for multiple DGs in an islanded MG. The key contributions in this paper are summarized as follows: The proposed two-step prediction FCS-MPVC for single DG in the islanded mode of MG. Discuss the results of single DG with the proposed control technique under different loading conditions and shows that the proposed controller has improved both steady-state response and transient response. The droop control is employed for accurate power-sharing between the DGs in AC MG. Moreover, the proposed control strategy capability is examined for multiple DG units. The real-time simulation is accomplished in the MATLAB/Simulink environment.

The rest of the paper is presented as follows: The proposed control strategy is explained and it provides the comprehensive mathematical model of two-level VSC with linked LC filter and the discretization aspects of FCS-MPC implementation are discussed in section II. Further, the FCS-MPC working and operation are explained in this section. In section III presents droop control and its boundaries. In Section IV, the detailed simulation results are presented. Finally, the last section comprises the conclusion.

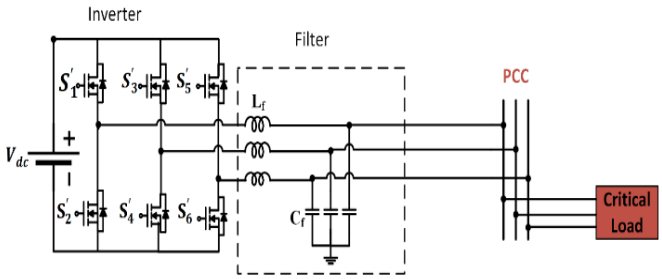

Figure 2. Circuit diagram of VSC having filter serving load at PCC.

II. MODELLING OF THE DER SYSTEM

Fig.1 shows that three VSIs are connected with a common ac bus through a transmission line with impedance and serving local loads. This section explained the proposed system configuration in which VSCs work and describe the discrete-time converter and its filter model which is used by MPC to find the optimal action by minimizing the CF and optimal control action is anticipated for next sampling time. A precise mathematical model of VSC and filter is required to attain adequate control performance. Mainly in AC MG, two-level VSC topology is used and, as shown in Fig. 2 and also presents a constant dc source that is connected with VSC. The output LC filter is used to eliminate the high-frequency components, which are undesirable.

VSC modelling is done in the stationary orthogonal frame of reference. The following initial conditions are considered: the VSC is in a balanced state. Three phases x-y-z are transformed into αβ frame by using Clarke transformation X:

$$\bar{v}=v_\alpha+jv_\beta=\bar{T}[v_x,v_y,v_z] \quad (1)$$

$$\bar{i}=i_\alpha+ji_\beta=\bar{T}[i_x,i_y,i_z]' \quad (2)$$

$$\bar{T}=\frac{1}{3}\left[1 \; e^{j\frac{2}{3}\pi} \quad 1 \; e^{j\frac{4}{3}\pi}\right] \quad (3)$$

A. Converter Model

It consists of three legs (S_x,S_y,S_z) and each leg has two switches, so there are two possible switching states for each leg, which are described below:

$$S_x=\left\{\begin{matrix}1, \text{ if } S_1' \text{ is ON and } S_4' \text{ is OFF}\\ 0, \text{if } S_1' \text{ is OFF and } S_4' \text{ is ON}\end{matrix}\right\} \quad (4)$$

$$S_y=\left\{\begin{matrix}1, \text{ if } S_2' \text{ is ON and } S_5' \text{ is OFF}\\ 0, \text{if } S_2' \text{ is OFF and } S_4' \text{ is ON}\end{matrix}\right\} \quad (5)$$

$$S_z=\left\{\begin{matrix}1, \text{ if } S_3' \text{ is ON and } S_6' \text{ is OFF}\\ 0, \text{if } S_3' \text{ is OFF and } S_6' \text{ is ON}\end{matrix}\right\} \quad (6)$$

However, two-level VSC has eight possible switching arrangements. the voltage between N point and leg can be computed by taking the product of dc-link voltage with the present state of the corresponding leg:

$$\begin{aligned}v_{xN}&=S_x.v_{dc}\\ v_{yN}&=S_y.v_{dc}\\ v_{zN}&=S_z.v_{dc}\end{aligned} \quad (7)$$

To find the voltage between phase to neutral (from x, y, z to n point) by subtracting the common voltage from (6). A common voltage is determined by applying the concept of Kirchhoff's voltage law:

$$v_{nN}=\frac{v_{xN}+v_{yN}+v_{zN}}{3} \quad (8)$$

Phase voltage is:

$$v_{xn}=v_{xN}-v_{nN} \quad (9)$$

$$v_{yn}=v_{yN}-v_{nN}$$

$$v_{zn}=v_{zN}-v_{nN}$$

Clark transformation is applied to find eight possible switching states. Which are shown in Table 1.

Table 1. Switching arrangement of VSI.

Space-Vector		On-state switches	Vector placing
Zero Vector	$\overrightarrow{V_{0,7}}$	S_1', S_3', S_5' S_4', S_6, S_2'	$\overline{v_{0,7}}=0$
Active Vector	$\overrightarrow{V_1}$	S_1', S_6', S_2'	$\overline{v_1}=\frac{2}{3}v_{dc}$
	$\overrightarrow{V_2}$	S_1', S_3', S_2'	$\overline{v_2}=\frac{1}{3}v_{dc}+j\frac{\sqrt{3}}{3}v_{dc}$
	$\overrightarrow{V_3}$	S_4', S_3', S_2'	$\overline{v_3}=-\frac{1}{3}v_{dc}+j\frac{\sqrt{3}}{3}v_{dc}$
	$\overrightarrow{V_4}$	S_4', S_3', S_5'	$\overline{v_4}=-\frac{2}{3}v_{dc}$
	$\overrightarrow{V_5}$	S_1', S_5', S_4'	$\overline{v_5}=-\frac{1}{3}v_{dc}-j\frac{\sqrt{3}}{3}v_{dc}$

B. LC Filter

To eliminate the switching harmonics, an LC filter is coupled at the VSI's output terminal, as shown in Fig. 2. The filter is consisting of an inductor with an inductance L_f , damping resistance R_f having current i_f, and a capacitor with capacitance C_f and the voltage across the capacitor is v_{pc}. i_f and v_{pc} are the state variables in this system. The filter response is explained by (10) and (11). Eq (10) describes the inductive nature, and the capacitance nature of the filter is defined by (11). Both equations are stated as:

$$L_f\frac{di_f}{dt}=v_t-v_{PC}-i_fR_f \quad (10)$$

$$C_f\frac{dV_{pc}}{dt}=i_f-i_0 \quad (11)$$

$$\frac{d}{d}\begin{bmatrix} i_f \\ v_{PC}\end{bmatrix}=\mathbf{A}\begin{bmatrix} i_f \\ v_{PC}\end{bmatrix}+\mathbf{B}\begin{bmatrix} v_t \\ i_0\end{bmatrix} \quad (12)$$

$$\mathbf{A}=\begin{bmatrix} \frac{-R_f}{L_f} & \frac{-1}{C_f} \\ \frac{1}{C_f} & 0\end{bmatrix} \quad (13)$$

$$\mathbf{B}=\begin{bmatrix} \frac{1}{L_f} & \mathbf{0} \\ \mathbf{0} & -\frac{1}{c_f}\end{bmatrix} \quad (14)$$

C. Discrete-Time Modelling of Filter.

To implement the proposed control on the digital platform, the continuous-time state-space model is converted to discrete-time state-space model. Discretization techniques are usually used, but this study uses the zero-order hold (ZOH) technique. This technique provides the direct conversion of the CTSS model to the DTSS model for every sampling in stair-case inputs. In this paper, a couple of assumption is made such as the value of dc-link voltage (V_{dc}) is a constant. Eq (12) is converted into the discrete time mathematical model and is written as:

$$\begin{bmatrix} i_f(t_k+1) \\ v_{PC}(t_k+1)\end{bmatrix}=\mathbf{A_d}\begin{bmatrix} i_f(t_k) \\ v_{PC}(t_k)\end{bmatrix}+\mathbf{B_d}\begin{bmatrix} v_t(t_k) \\ i_0(t_k)\end{bmatrix} \quad (15)$$

$$\mathbf{A_d}=e^{AT_s} \quad (16)$$

$$\mathbf{B_d}=\int_0^{T_s} e^{A\tau}\,B\,d_\tau \quad (17)$$

T_s is sampling instant. It is assumed that T_s is very small so the exponential matrix is approximated as:

$$e^{AT_s}\approx 1+AT_s \quad (18)$$

By using (15), the capacitor voltage at instant (t_k+1) can be determined by the following equation:

$$v_{pc}(t_k+1)=v_{pc}(t_k)+\frac{T_s}{C_f}(i_f(t_k)-i_0(t_k)) \quad (19)$$

To regulate the capacitor voltage. The cost function is defined as:

$$g_v=(v^*_{pc,\alpha}(t_k)-v_{pc,\alpha}(t_k+2))^2+(v^*_{pc,\beta}(t_k)-v_{pc,\beta}(t_k+2))^2 \quad (20)$$

$v_{pc,\alpha}$ and $v_{pc,\beta}$ are real and imaginary parts of predicted capacitor voltage. Among all the voltage vectors, a vector that has a minimum value of g_v can be applied to the next sampling instant.

III. Droop Control

Originally each DG is designed to generate power according to its reference at the base frequency, i.e., 60 Hz in this study, In the case of Islanded MG, the main aim of the local controller of DG is to compensate the voltage and frequency within MG. But there is a need for the secondary controller to control the voltage and frequency of MG. Droop control is extensively adopted in MG to control the voltage and frequency and for proper sharing of active and reactive power between the DGs [12]. In this work, droop control is used for accurate sharing of the active and reactive power of each DG proportional to its ratings. Droop control can be expressed as follows:

$$V_{ref}=V_{nom}-k_qQ_{cal} \quad (21)$$

$$f_{ref}=f_{nom}-k_pP_{cal} \quad (22)$$

Where, V_{ref} and f_{ref} are reference voltage amplitude and frequency used to synthesis the $V_{ref,\alpha\beta}$. V_{nom} and f_{ref} are nominal voltage amplitude and frequency. Following equations are used to calculate the P_{cal} and Q_{cal} as:

$$P_{cal}=v_{pc,\alpha}i_{0,\alpha}+v_{pc,\beta}i_{0,\beta} \quad (23)$$

$$Q_{cal}=v_{pc,\beta}i_{0,\alpha}-v_{pc,\alpha}i_{0,\beta} \quad (24)$$

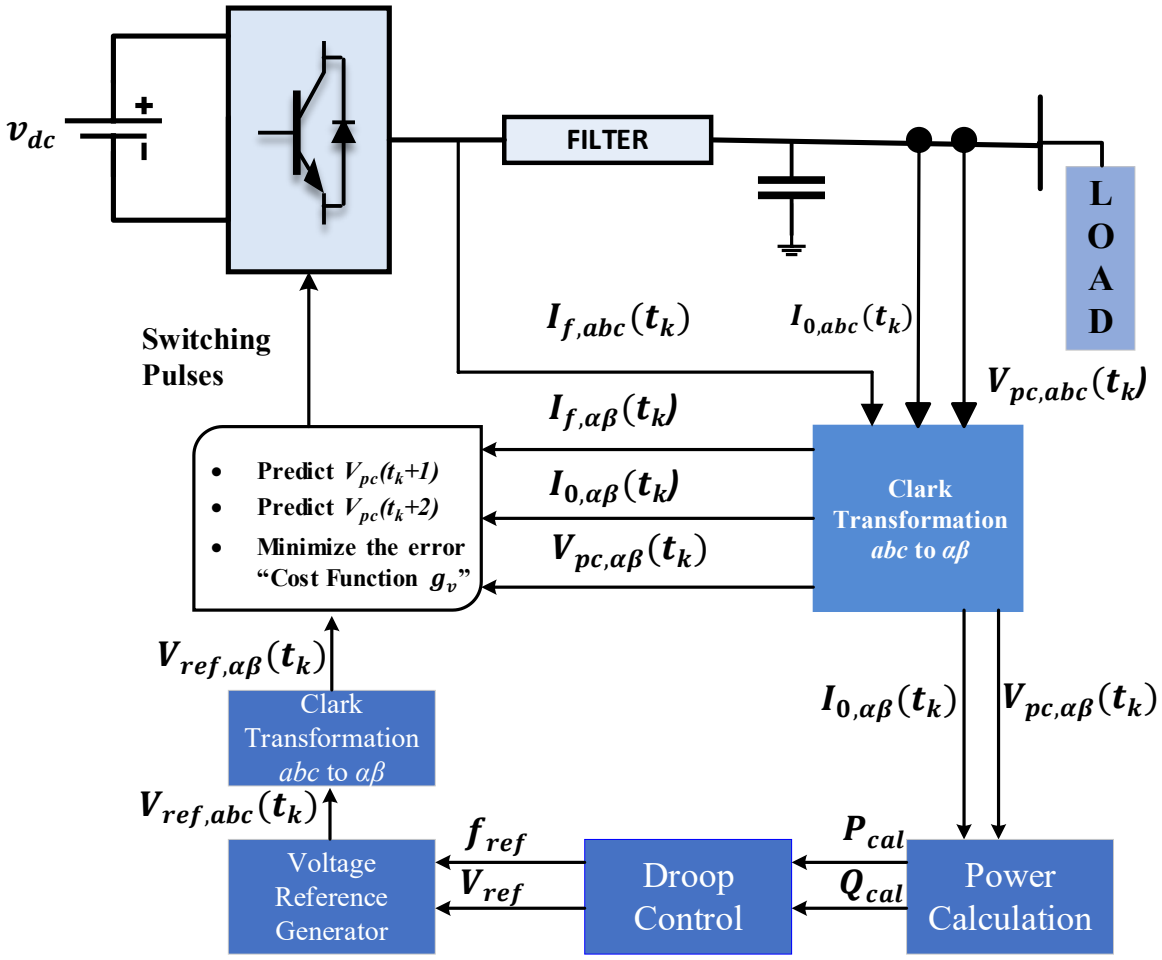

Figure 3. Block diagram of investigating control scheme along with droop control in islanded mode of MG.

Power can be determined by using (23) and (24) then it is processed through a lowpass filter to attenuate the oscillations. However, the lowpass filter has produced delays during transients. k_p and k_q are droop power coefficients. Voltage regulation and coefficients show an inverse relationship. So, there is a trade-off between them to find the best possible solution Droop curves is also based on voltage delta and coefficients of droop. Coefficients of droop is stated as:

$$k_q = \frac{\Delta V}{Q_{max}} \quad (25)$$

$$k_p = \frac{\Delta f}{P_{max}} \quad (26)$$

ΔV and Δf are extremely allocated divergence of voltage and frequency. Q_{max} and P_{max} are the maximum reactive and active power rating of the DER. The control technique expressed in (20) and (21) is normally known as conventional droop control, and it is fully decentralized. But it has several practical restrictions.

IV. SIMULATION RESULTS

For validation of control technique, extensive real-time simulations are carried out in MATLAB/Simulink for both single inverter and tested MG. Different simulations scenarios are performed to evaluate the capabilities under various load conditions. Different types of loads, such as linear and non-linear loads, are considered in this study. The linear load consists of a three-phase RL load with the active and reactive power demand of P= 18 kW and Q= 7 kvar.

In order to verify the claimed novelties such as the response of the proposed control approach and its robustness, scenario-based simulation is done in MATLAB/Simulink. First of all, the performance of DER with the proposed controller is verified under the steady-state condition, and voltage reference is a sinusoidal wave. Afterwards, Different tests, such as linear and non-linear loading condition, disturbance in the system due to change of load, are performed to verify the stability and robustness of the controller. In the end, two DERs are working in parallel along with the proposed controller in the inner loop and droop control is implemented as part of primary control of MG. Droop control is used to share accurate power between the DGs. Fig. 3 demonstrates the whole implementation of proposed control technique for single DG in AC MG.

Table 2. Simulation Parameters.

DC link Voltage	v_{dc}=1000V
Sampling Time	T_s=20μs

LC-filter	C_f=250μF,L_f=2mH
Damping Resistance	R_f=0.94Ω
Linear load	P=18kW,Q=7kVar
Non-linear load (diode rectifier)	P=10kW,Q=4kVar
Nominal Voltage	V_{nom}=318V
Rated Frequency	f_{nom}=60Hz
Droop coefficients	k_q=0.001,k_p=0.001

A. Steady-State Analysis

Fig 4 illustrates the result of a DER under normal conditions when linear RL load is connected. DER supplied the 18-kW active and 7 kVar reactive power to meet the load demand. The frequency of the MG is 60 Hz and the RMS voltage are set to 220V. Load current and voltage are sine waves with little harmonics. The THD of the voltage in this study is 0.90 %, which is within the acceptable limit of IEEE criteria. It is also compared with standard literature, in which MPVC is implemented for two level inverter and 2.93 % is Voltage THD found under linear load in [13]. . In order to test the performance of the controller under non-linear load. The results of non-linear load connected with the system is illustrated in Fig. 5. Due to non-linear load, the current of DG becomes distorted but the voltage remains sine wave with the THD of 1.23%. So, the investigating scheme easily handles the non-linearity of the system.

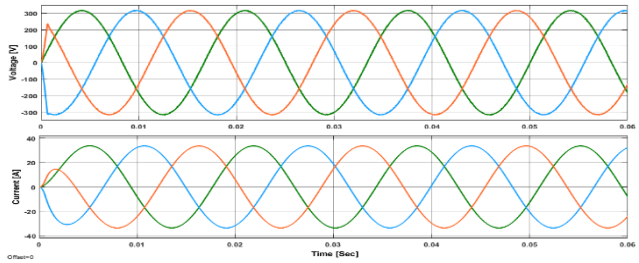

Fig.4. Load current and output voltage of single DG under linear load.

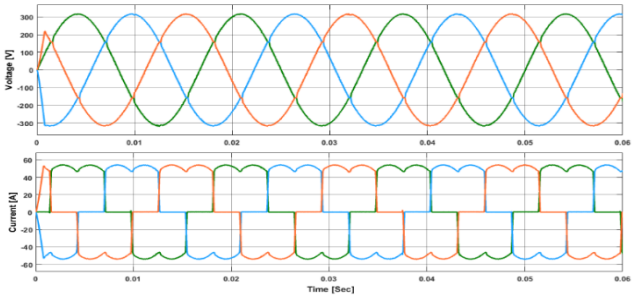

Fig.5. Load current and output voltage of single DG under nonlinear load.

B. Load Tresients Study

In this section, the load transient performance is evaluated to determine the system transient response and overshoot under varying load conditions from 100% load to 0% load and vice versa. Fig. 6 demonstrates the controller response under sudden change of load from no load to full load and vice-versa. It is seen from the results at time t=0.03s total load is disconnected from the bus and now the system is under no-load condition. Again, at the time, t= 0.04s all load is again connected to the system, but during the whole time, the output voltage of the system remains unaffected.

The same test is performed for the non-linear load. Fig. 7 shows that at time t=0.03s load is disconnected from the system, and it becomes under no-load condition. But it is noticed that output voltage shows a spike and remains sinusoidal., The performance of the proposed controller under various loading conditions are tested and verified through the simulations results.

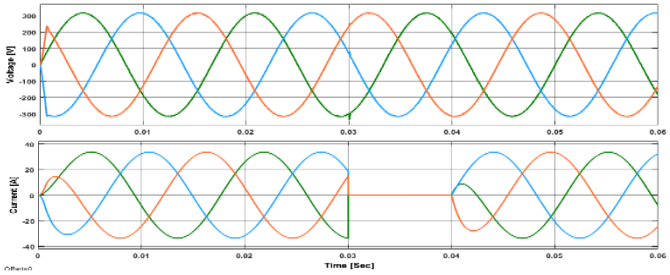

Fig. 6. Output voltage and load current under linear load variations.

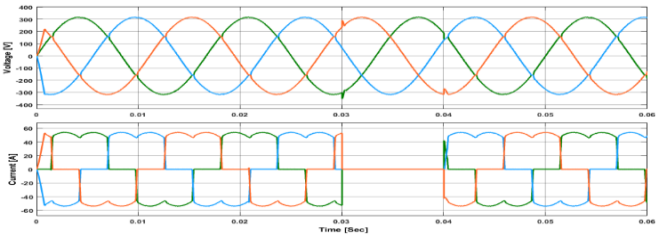

Fig. 7. Output voltage and load current under non-linear load transients.

C. Multiple DGs: Results and Discussion

After validation of proposed control for single DER, this technique is finally developed for two inverters connected in parallel to serve an available load, and simulation is done in MATLAB/Simulink environment. The results are discussed below. At the same time, classical droop-control is also implemented at the upper level of primary control to share the proper power among the DERs. To increase the system stability and for cost reduction, different rating DG are connected together in MG. The features of power-sharing and load transients are investigating. Power-sharing among the inverters are presented in Fig. 8. It expressed that active and reactive power sharing among the DGs. At time t= 0.03s, power demand becomes double. In order to meet load demand, both DGs immediately increase their power production. Fig. 8 (a), (b), (e), and (f) illustrate the resulted current and voltage of DG_1 and DG_2. It is to be shown that at t=0.03s due to an increase in demand, the current of both inverters increases, and voltage remains throughout the time. The droop equally shares active and reactive power because both DGs are of equal rating. All simulation results verify that MPC is more robust and far superior to any other classical linear controller. Table 3 explains the comparison in terms of THD and controller complexity among non-linear and linear control techniques. The presented control technique has a better transient response, low voltage THD, and has the capability to handle the nonlinearity.

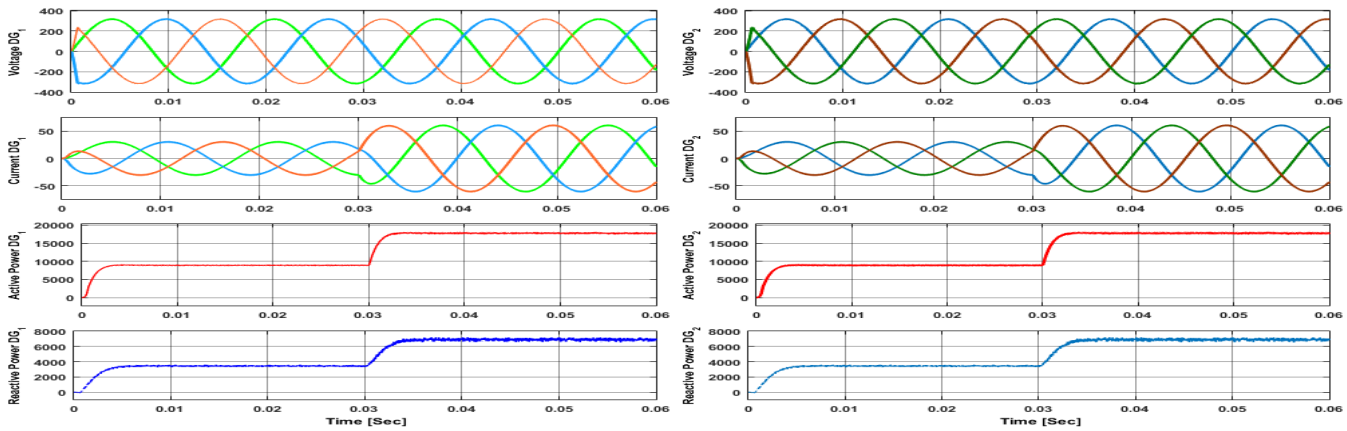

Fig. 8. voltage, load current, active and reactive power of both DG_1 and DG_2 under load transients.

Table 3. Comparison of different control methods.

References	Techniques Implemented	Voltage Quality with Linear-Load (THD)	Voltage Quality with NonLinear-Load (THD)	Implementation Complexity
[14]	Proportional Integral	16	42	Low
[15]	Dead-beat	2.1	4.8	Medium
[16]	Proportional Resonant	1.4	4.6	Low
[17]	Slide Mode Control	--	2.66	High
[18]	Classical MPC	5.1	6.7	High
[9]	Observer based MPC	2.82	3.8	Medium
[13]	Implicit based MPC	2.93	Not studied	Medium
Proposed	**Improved FCS-MPC**	**0.90**	**1.23**	**Medium**

V. Conclusion

The improved FCS-MPC based voltage control has been studied for single and multiple DERs in AC MG. The performance of the proposed predictive controller has been verified by executing the various simulations in the MATLAB/Simulink. Simulation results demonstrate that the proposed controller attains excellent voltage regulation under linear loads and non-linear loads. The proposed controller doesn't need any external or internal parameters for adjustment. It only requires the system model to predicts the controlled variables. Additionally, no modulator is required. Thus the gate signals are directly provided by the controller. The proposed controller offers flexibility and eliminates the cascaded configuration to control output voltage directly. Droop control is implemented for accurate power-sharing among the DGs. The results verify the response and effectiveness of droop-control to share the proper power among the DERs in both steady-state and transient conditions under linear and non-linear loading conditions.

Acknowledgment

This work is carried out by the financial support provided by the Walter Ahlström Foundation Finland with grant # 2021/40.

Some parts of this work are done in the SolarX research project with the financial support provided by Business Finland with Grant No. 6844/31/2018. The financial support provided through these funding organizations is highly acknowledged.

References

1. Saad, W., et al., *Game-theoretic methods for the smart grid: An overview of microgrid systems,demand-side management, and smart grid communications.* IEEE Signal Processing Magazine, 2012. **29**(5): p. 86-105.
2. Madureira, AG and J.P. Lopes, *Coordinated voltage support in distribution networks with distributed generation and microgrids.* IET renewable Power generation, 2009. **3**(4): p. 439-454.
3. Tavakoli, A., et al. *A decentralized control strategy for multiple distributed generation in islanded mode*. in *PES General Meeting| Conference & Exposition, 2014 IEEE*. 2014. IEEE.
4. Dragičević, T., et al., *DC microgrids—Part I: A review of control strategies and stabilization techniques.* IEEE Transactions on power electronics, 2016. **31**(7): p. 4876-4891.
5. Liu, X., P. Wang, and PC. Loh, *A hybrid AC/DC microgrid and its coordination control.* IEEE Transactions on smart grid, 2011. **2**(2): p. 278-286.
6. Golestan, S., J.M. Guerrero, and J.C. Vasquez, *A PLL-Based Controller for Three-Phase Grid-Connected Power Converters.* IEEE Transactions on Power Electronics, 2018. **33**(2): p. 911-916.
7. Blaabjerg, F., et al., *Overview of control and grid synchronization for distributed power generation systems.* IEEE Transactions on industrial electronics, 2006. **53**(5): p. 1398-1409.
8. Ali, M., et al., *Lyapunov Stability and Performance Analysis of the Fractional Order Sliding Mode Control for a Parallel Connected UPS System under Unbalanced and Non-linear Load Conditions.* Energies, 2018. **11**(12): p. 3475.
9. Cortés, P., et al., *Model predictive control of an inverter with output $ LC $ filter for UPS applications.* IEEE Transactions on Industrial Electronics, 2009. **56**(6): p. 1875-1883.
10. Ahmed, K.H., et al., *A modified stationary reference frame-based predictive current control with zero steady-state error for LCL coupled inverter-based distributed generation systems.* IEEE Transactions on Industrial Electronics, 2011. **58**(4): p. 1359-1370.

11. Khan, H.S., et al., *Finite Control Set Model Predictive Control for Parallel Connected Online UPS System under Unbalanced and Non-linear Loads.* Energies, 2019. **12**(4): p. 581.
12. Sao, C.K. and PW. Lehn, *Autonomous load sharing of voltage source converters.* IEEE Transactions on Power Delivery, 2005. **20**(2): p. 1009-1016.
13. Nauman, M. and A. Hasan, *Efficient implicit model-predictive control of a three-phase inverter with an output LC filter.* IEEE Transactions on Power Electronics, 2016. **31**(9): p. 6075-6078.
14. Sun, X., Y.-S. Lee, and D. Xu, *Modeling, analysis, and implementation of parallel multi-inverter systems with instantaneous average-current-sharing scheme.* IEEE Transactions on Power Electronics, 2003. **18**(3): p. 844-856.
15. Mattavelli, P., *An improved deadbeat control for UPS using disturbance observers.* IEEE Transactions on Industrial Electronics, 2005. **52**(1): p. 206-212.
16. Hasanzadeh, A., et al., *A proportional-resonant controller-based wireless control strategy with a reduced number of sensors for parallel-operated UPSs.* IEEE Transactions on Power Delivery, 2010. **25**(1): p. 468-478.
17. Komurcugil, H., *Rotating-sliding-line-based sliding-mode control for single-phase UPS inverters.* IEEE Transactions on Industrial Electronics, 2011. **59**(10): p. 3719-3726.
18. Yaramasu, V., et al., *Model predictive approach for a simple and effective load voltage control of four-leg inverter with an output $ LC $ filter.* IEEE Transactions on Industrial Electronics, 2014. **61**(10): p. 5259-5270.